J. Ind. Geophys. Union, 30(1) (2026), 59-69
https://doi.org/10.71122/JIGU.30(1)2026.006

Fault plane solutions of the earthquakes (1.8≤ M_L ≤ 3.5) in the Himachal Himalaya, India

Ankush Kumar Ruhela*, J. Das and S.C. Gupta
[1] Department of Earthquake Engineering, Indian Institute of Technology Roorkee,
Roorkee- 247667, India
*Corresponding author: aruhela@eq.iitr.ac.in

ABSTRACT

It is widely acknowledged that even when earthquakes occur inside a specific confined area, there can be significant variations in the focal mechanism solutions. Several earthquakes have been detected by broadband seismometers coupled with a digital recorder (Centaur) at six stations in the Himachal Himalaya during 2018-2019. Therefore, we addressed an approach for identifying the orientation of fault planes in the studied area. In this paper, we retrieved the fault plane solutions of 25 earthquakes using a double couple fault plane method, based on P-wave polarity readings and amplitude ratio with the help of the Seisan program. Earthquakes exhibit diverse fault plane solutions. From a total of 25 earthquakes, 3 show normal faulting, 19 show reverse faulting, and 3 show strike-slip mechanism. This is because rupture lengths for local events (M < 3.5) are typically in the range of a few hundred meters to a kilometer, and events may occur on faults with varying orientations. The maximum concentration of thrust faults is consistent with the trend of the Himalayan collisional zone and the location of major faults. Except for some showing a dip greater than 60°, earthquakes with precisely measured depths characterise a zone from 0.1~25 km with an average dip of about 44.6°. All focal mechanisms of events that are available within this zone, indicate a steeper dip. An earthquake that occurred near the Sundarnagar fault, shows a strike-slip mechanism. Based on this interpretation, there may be a genetic relationship between the Himalayan block above the MBT and a transverse structural feature in the underthrusting Indian plate (Sundarnagar fault). Earthquakes reveal a trend of directions concerning the T-axis and P-axis with all types of fault plane solutions.

Keywords: Earthquake, Fault plane solution, Geology and tectonics, Underthrusting, Himachal Himalaya region.

INTRODUCTION

The nature of the instantaneous faulting or earthquake process is one of the most substantial and engaging issues in seismology. The triggering mechanism and the natural mechanism of elastic strain concentration are the fundamentals of earthquake kinematics. Conventionally, the term “fault plane solution” (FPS) relates to the fault orientation, the patterns of stress release, and displacement direction, as well as the dynamic mechanism of seismic wave propagation. The FPS explains the pattern and geometry of faulting following an earthquake. The fault geometry affects the radiated amplitudes in various azimuthal directions, therefore, the FPS is derived from the polarity of the first motion or the amplitude of seismic waves. There is a persuasive explanation that the progressive stresses caused by plate movements, affect specific regions of the Earth’s crust and the upper mantle. When stressed rocks suddenly fracture, strain and stress are released simultaneously, which produce seismic waves or earthquake waves. Abrupt fractures typically happen at weak spots in the stressed rocks. The blocks that move in opposite directions due to shear motion on either side of the fault plane, or fracture plane, are referred to as fractures. Since shear motions do not entail a volume change, they can happen anywhere in the brittle region of the Earth's outermost layers, even at significant depths in the upper mantle in some circumstances, where the pressure is quite high. These findings demonstrate that several events with various focal mechanism solution orientations can take place even within a very small region with a few kilometers in dimension. Teleseismic observations from the global network in the 1960s provided sufficient data to determine focal mechanisms for strong and medium-sized earthquakes that were successfully used to formulate the general theory of plate tectonics (Isacks et al., 1968). During the last 15 years, the availability of dense portable networks has permitted the field study of regional micro-seismicity, aftershocks of large earthquakes, swarms, and volcanic events. The methods used for global studies were transferred to local problems without basic modifications. Nevertheless, even in the case of a large number of seismic stations, it is difficult to set up a local network surrounding the focal sphere satisfactorily.

The tangential traction at the interface between two bodies can be inferred from their relative motion. It would be feasible to draw conclusions about the regional stress field if the tangential traction in a given area could be recognised on a variety of planes. A sudden physical change of the ground during an earthquake, releases the accumulated elastic energy. The two blocks of a fault move in opposition to one another, which results in first P motion with distinct polarities in various directions. It would be easy to identify the orientation of the two planes if the measurements from numerous equally dispersed stations around the epicenter were available by partitioning the area into four quadrants with different polarities. However, there is no way to differentiate between the fault plane and the auxiliary plane without additional information. The double-couple source method relies on this inherent ambiguity. To identify the fault plane, there are a few different approaches. A surface break on a fault caused by an earthquake must match one of the planes in the mechanism solution for the displacement and fault plane that were observed. Different approaches must be used because the majority of earthquakes do not coincide with a surface break on land. In order to demonstrate that the slip was consistent over broad regions if it occurred in the fault plane as opposed to the auxiliary plane. McKenzie and Parker (1967) employed the horizontal projection of the slip vector to eliminate the ambiguity. Other possible sources of information include, the aftershock distribution, the radiation pattern as a function of frequency, and the ellipticity of the isoseismal lines. Various authors (Hodgson, 1957; McIntyre and Christie, 1957; Scheidegger, 1964; Shirokova, 1967) have emphasized the significance of a direction, such as the P or T axis or the null-motion direction, that is exclusively indicated by the fault-plane solution. There is no physical evidence to support this idea because the ambiguity depends on the use of distant stations and is not a characteristic of the fault motion. It is evident from the success of the ideas of paving stone tectonics (McKenzie and Parker, 1967; Morgan, 1968) that selecting between the fault plane and the auxiliary plane, is essential. The ambiguity between the fault and the auxiliary planes can be resolved with additional information from tectonics and aftershock activity data. The faults can be classified as thrust faults, normal faults, and strike-slip faults based on the nature of relative movement along the fault. Hauksson (1990) defined normal-slip vectors with rakes between -45˚ and -135˚, reverse-slip vectors with rakes between 45˚ and 135˚, and strike-slip vectors with rakes between 44˚ and -44˚. Classifications of fault types along these lines are outlined in the Table 1.

Numerous authors have long explored focal mechanism solutions of earthquakes (Honda et al., 1956; Stauder, 1964; Wickens and Hodgson, 1967; Isacks and Molnar, 1971). Lately, a variety of polarity data of P wave beginning motions acquired by dense seismic networks have also been used to infer focal mechanism solutions for small events (Ishida, 1992; Yarnazaki et al., 1992; Castillo and Ellsworth, 1993; Ndikum et al., 2014). These findings demonstrate that numerous occurrences with various focal mechanism solution orientations can be found even within a confined area with dimensions of a few kilometers.

GEOLOGY AND TECTONICS OF THE HIMACHAL HIMALAYA

Himalaya is one of the seismically active regions in the globe where severe earthquakes keep on occurring on a regular basis. Although a trend has been identified, the seismicity in the Himalaya appears to be non-uniform due to the very short instrumental record. This trend is related to a narrow belt of intermediate events between the Main Central Thrust (MCT) and Main Boundary Thrust (MBT), that lies beneath the Lesser Himalaya (Barazangi and Ni, 1982). Being formed as a result of the collision of the Asian and Indian continents, the Himalaya was taken into consideration. According to Dewey and Bird (1970), the Himalaya was created by the collision of the Indian and Asian continents, surrounded by a marginal trench. They believed that further subduction was precluded by the buoyancy of the lithosphere convergence. Powell and Conaghan (1973) made modifications to Dewey and Bird (1970) continent-continent collision model, since such a collision cannot account for the formation of the present-day Himalaya. They put forth an evolutionary theory with two orogeny phases. The Cretaceous to early Tertiary (Eocene) subduction zones along the Indus-Tsangpo suture zone (ITSZ), where India and Asia collided, are related to the first phase. This phase came to an end in the Eocene, and the collision that caused the ITSZ is its immediate aftereffect. The second phase includes the emergence of intracontinental fractures inside the Indian continent and the underthrusting of the Indian continent beneath the Himalaya from the Miocene to the present time.

In the Miocene, an intracontinental main central thrust (MCT) formed south of the suture zone, and in the Pliocene, an intracontinental main boundary thrust (MBT) occurred even further south. The convergence is focused on the newest of these structures at each stage.

Table 1. Classification of fault type based on rake angle (Cronin, 2010).

S.No.	Rake	Fault type
1	0˚ or 180˚	Pure strike-slip fault
2	90˚	Pure reverse fault
3	-90˚	Pure normal fault
4	-20˚ to 20˚	Left-lateral strike-slip fault
5	20˚ to 70˚	Reverse left-lateral oblique
6	70˚ to 110˚	Reverse fault
7	110˚ to 160˚	Reverse right-lateral oblique
8	-160˚ to 160°	Right-lateral strike-slip fault
9	-110° to -160°	Normal right-lateral oblique
10	-70° to -110°	Normal fault
11	-20° to -70°	Normal left-lateral oblique

The MCT and MBT are tectonically analogous faults of various ages in the evolutionary model. While the MCT has been dormant for over 15 million years, the MBT is now operational. In the steady-state model, the Indian Plate moved northward by underthrusting its leading edge rather than stacking behind the Himalaya when the Tethys ocean was closed along the ITSZ. There are not many differences between this form of continental subduction and oceanic subduction. Because of this, the MCT is active in the steady state model while being dormant in the evolutionary model.

Numerous plate tectonics models for the progression of the Himalaya were introduced as more evidence became available (Lefort, 1975; Molnar et al., 1977; Bird, 1978; Seeber et al., 1981; Barazangi and Ni, 1982). According to the reports, the Siwalik Himalaya, Lesser Himalaya, High Himalaya, and Tethyan Himalaya are the tectonostratigraphic domains of the Himalaya, running from south to north. Sediments from the Cambrian and Eocene make up the Tethyan Himalaya, which are rich in fossils. The MCT divides the High Himalaya from the Lesser Himalaya. The shift in the folding and metamorphism grade and style of structures is what defines the thrust. Since the middle of the Tertiary (Miocene), the MCT has been evolving. Granite and metamorphic rocks make up the High Himalaya. Some people referred to it as the central crystalline zone. The MBT divides the Lesser Himalaya from the Siwalik Himalaya. Since the Pliocene, the thrust has grown. Sedimentary rocks that have undergone metamorphosis and small amounts of volcanic rock, make up the Lesser Himalaya. These rocks also include transported, isolated fragments of central crystalline rocks. The main frontal thrust (MFT) separates the Indo-Gangetic Plain from the Siwalik Himalaya. Sandstone and mudstone are found in sequence throughout the Siwalik zone.

There have been four great Himalayan earthquakes ($M_w \geq 8$) previously: the 1897 Shillong earthquake ($M_w \geq 8.2$), the 1934 Bihar-Nepal earthquake (M_w- 8), the 1950 Assam earthquake (M_w- 8.6), and the 1905 Kangra earthquake (M_w- 7.8). There are several large magnitude ($M_w \geq 7$) earthquakes as well: the 2005 Kashmir earthquake (M_w-7.6), the 2015 Gorkha earthquake (M_w-7.8), and the 2015 Dolakha earthquake (M_w-7.3). The noticeable earthquakes that have happened in the vicinity of the research area over the past 120 years include, the 1905 Kangra earthquake (M_w-7.8), the 1945 Chamba earthquake (M_s~6.5), the 1975 Kinnaur earthquake (m_b~6.2), and the 1986 Dharamshala earthquake (m_b -5.5). Molnar and Deng (1984) reported the fault plane solution for the Kangra earthquake as a reverse faulting with a dip of 5°, strike 300°, rake $90^\circ$and focal depth of 15 km. Molnar and Chen (1983) reported the fault plane solution for the Kinnaur earthquake as normal faulting with a strike-slip component having a dip of 40°, strike 180°, rake 270°, and a focal depth of 9 km. In addition to these, the Garhwal Himalaya was the site of the 1991 Uttarkashi earthquake (M_w-6.7) and the 1999 Chamoli earthquake (M_w-6.5). Cotton et al. (1996) discovered the hypocentre at a depth of 14 km with a strike angle of 318°, dip angle of 11°, and rake angle of 114° for the Uttarkashi earthquake. Xu et al. (2016) reported the fault plane solution for the Chamoli earthquake as reverse faulting with a dip of 9°, strike 292°, rake $90^\circ$and focal depth of 15 km. The studied region is situated in the Himachal Himalaya, which contains the Himalaya's northwest region. Additionally, the studied area is characterized by the presence of local and regional tectonic features, including the Drang thrust (DT), the Ropor fault, the Reasi thrust, the Jawalamukhi thrust (JMT), the Sundarnagar fault (SNF), the Kistwar fault (KF), the Kaurik fault system (KFS), the Alakhnanda fault (AF), and the Brasar thrust. Several subsidiary thrusts, including Jwalamukhi and Drang thrusts, which have a significant spatial extent, intersect the frontal belt (between the MBT and the MFT). Figure 1 illustrates the geography of the local network of six stations installed in the Himachal Himalaya. The earthquake data are used to study the focal mechanisms and attributes of the seismic source of the region. Table 2 shows the geographical coordinates and altitudes of the recording sites.

DATA ACQUISITION

For the present study, a network has been set up around the proposed area to study the focal mechanisms of earthquakes. The digital seismographs, consisting of a short-period triaxial seismometer (20-sec compact trillium at four stations) and broadband triaxial seismometer (120-sec trillium at two stations), coupled with a digital recorder (Centaur), have been used for the recording of local earthquakes at the stations during 2018-2019. Digital data is recorded at 100 samples per second. A total of 25 local earthquakes have been identified and are considered for the study of focal mechanisms. All local events are located in the Lesser and High Himalaya. A global positioning system is included with digital stations to synchronize data to IST or UTC. The FPS of events have been drawn, based on amplitude ratios and polarities of the vertical P-wave motions. Figure 2 illustrates the time history of an event at six stations along with the ground motion.

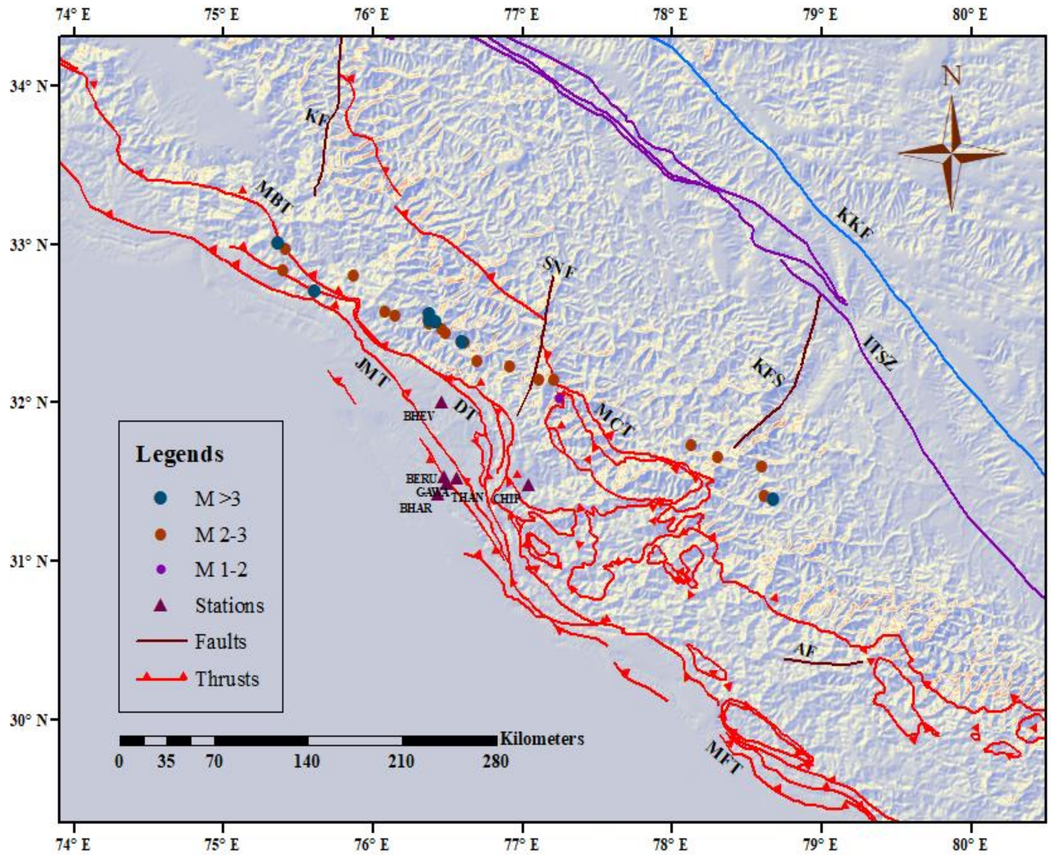

Figure 1. Map showing the study area, the tectonic features in the Himachal Himalaya with events (circles), and locations of seismic stations (triangles). KKF- Karakoram fault, ITSZ- Indus Tsangpo suture zone, KFS- Kaurik fault system, MCT- Main central thrust, MBT- Main boundary thrust, MFT- Main frontal thrust, JMT- Jwalamukhi thrust, DT- Drang thrust, SNF- Sundarnagar fault, AF- Alakhnanda fault, KF- Kishtwar fault, (Tectonic features are from Seismotectonic Atlas of India and its Environs by GSI (2000), along with SRTM-DEM).

Table 2. Geographical coordinates of the recording stations.

S. No.	Station name	Station code	Lat (°N)	Long (°E)	Elevation (m)
1.	Thana Plaun	THAN	31.49	76.50	736
2.	Gawali	GAWA	31.52	76.56	1692
3.	Bharoti	BHAR	31.42	76.44	1176
4.	Chhiprum	CHIP	31.48	77.04	2009
5.	Beru	BERU	31.53	76.48	913
6.	Bhevelli	BHEV	32.00	76.46	1525

METHODOLOGY

To monitor the earthquake activity around the studied area with specific objectives, it is necessary to have an optimum aperture of the network that encompasses the area spatially and azimuthally. The network was deployed by the Department of Earthquake Engineering, IIT, Roorkee. The events have been recorded digitally by the stations, and the phase data of these events have been used in the study. These data sets of local events have been used to locate hypocenters and to study FPS. The hypocenter parameters of 25 local events were estimated by employing the HYPOCENTER program (Lienert and Havskov, 1995), which is incorporated into the Seisan software (Havskov and Ottemoller, 2003). Because the understanding of the local velocity model of the region defined by the network, is an important requirement, the velocity model given by Chander et al. (1986) (Table 3) and modified by Kumar et al. (1994) for the Garhwal Himalaya region, is used in the present study to locate the events. This velocity model is also applicable to the Himachal Himalaya. The standard errors in the estimation of the epicenter (ERH), focal depth (ERZ), and origin time (RMS) are ERH ≤ 5.0 Km; ERZ ≤ 5.0 Km; and RMS ≤ 0.50 s. Tables 4 list the hypocentre parameters of 25 local events.

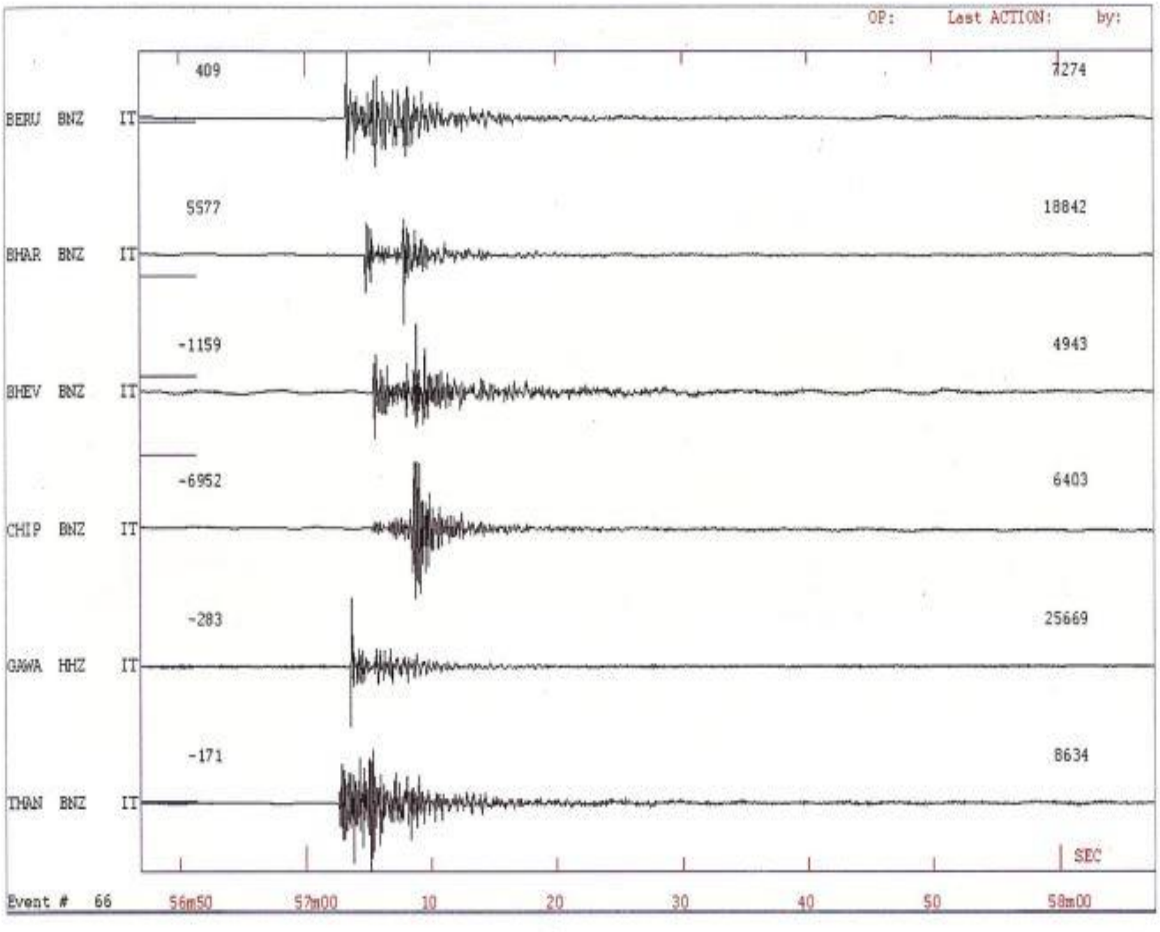

Figure 2. Example of an earthquake 5event recorded at six stations.

Table 3. Velocity model used for locating local earthquakes.

S. No.	P-wave velocity (km/s)	Depth to the top of the layer (km)
1	3	0
2	5.2	1
3	6	16
4	7.91	46

The amplitudes and polarities of the vertical P-wave motion of more than six stations are used to determine the FPS of aa the events that occurred in the Lesser and High Himachal Himalaya. The computer program FOCMEC_EXE has been utilized to calculate FPS (Snoke et al., 1984). This initiative is a component of the SEISAN software (Havskov and Ottemoller, 2003). The polarities and amplitude ratios of identical direct waves are utilized as the program's input data. The amplitude ratios are utilized to constrain the solutions, while the polarities yield the FPSs. The FOCMEC_EXE program requires two information, the maximum number of polarities and the amplitude ratio error, which should be less than a given ratio error. If there are a few badly distributed data points, changing one parameter can give a distinct result. In this study, the guiding criteria of local events for the FPS study include the number of stations that recorded an event and the geographical distributions of stations around MBT and MCT. Because it has been noted that many earthquakes fulfil this requirement, the minimal number of stations needed is set at 6.

The number of polarity errors is decided based on the values of the available data, and the value of 2 is picked from the proposed range of 0 to 5. The value of 0.1 is utilized for the maximum amplitude ratio inaccuracy. Errors are within 10%, according to this ratio. First, the P-wave recorded at different stations can show either compression or dilation first motion, depending on whether the initial motion is toward or away from the source. A zone of compression appears ahead of a fault, and a zone of dilatation appears behind it when the initial motion of the fault is directed towards the station. This would be converted into motions up or down on a vertical component sensor, accordingly. When the direction of the first motion was on the auxiliary plane, the same pattern of compression and dilatation would have been observed. After plotting P-wave, S-wave, and amplitude data, the program performs the input data to create an effective and methodical grid search for a focal sphere. The program was used to produce possible fault-plane solutions, giving rise to the possibility of presenting several solutions. A program was then used to plot the resultant solution, yielding the fault plane solution in a beach-ball representation (Figure 3).

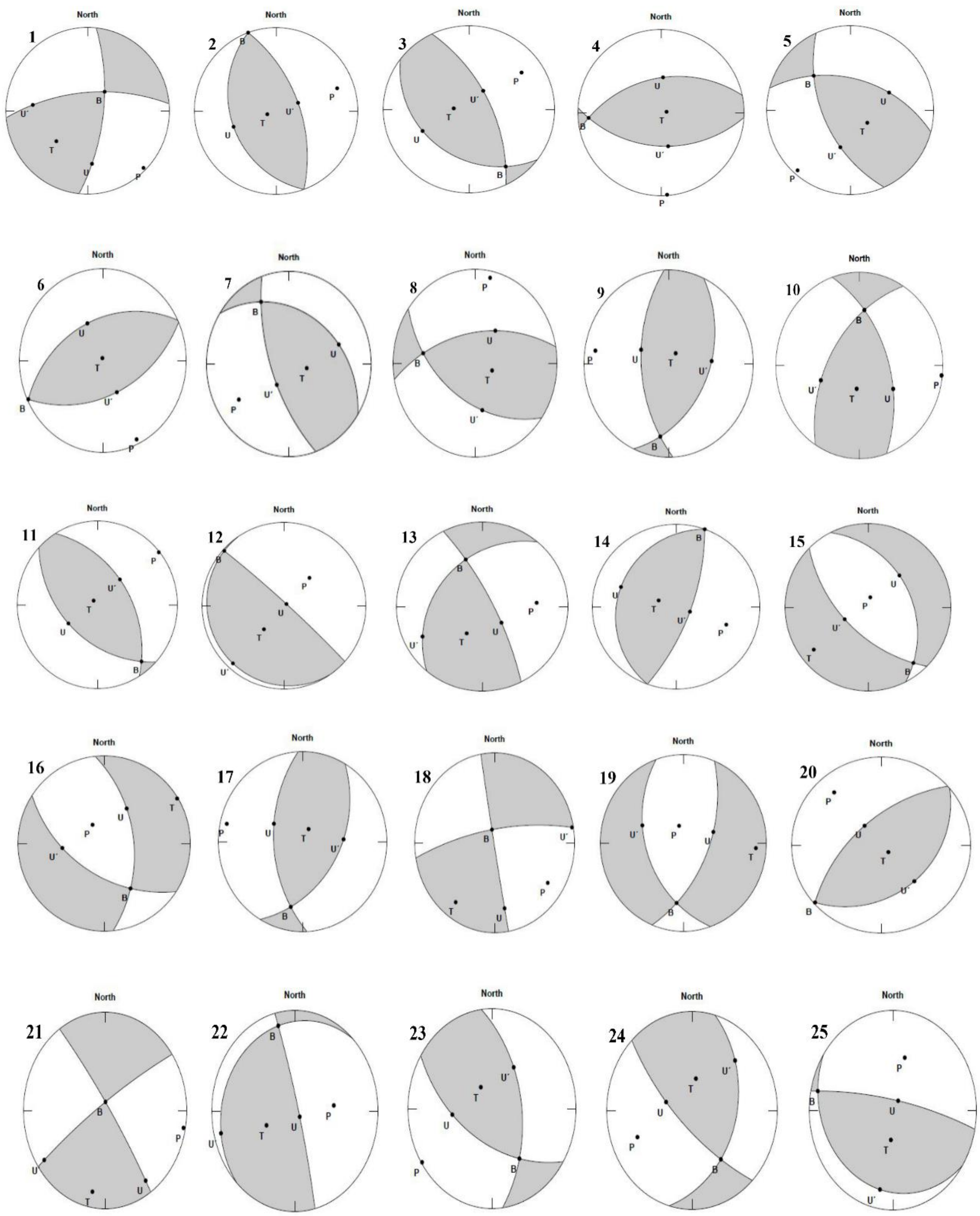

Figure 3. Beach-ball representation of the fault-plane solution of the 25 studied events.

Table 4. Hypocenter parameters of 25 local earthquakes in the Himachal Himalaya from November 2018 to March 2019.

S. No	Date (YYMMDD)	Org time HR:MN:SS	Lat (ºN)	Long (ºE)	Local mag. (M_L)	RMS Sec	ERH Km	ERZ Km
1	20181103	11:08:08.2	31.41	78.62	2.3	0.2	1.4	2.4
2	20181111	21:50:09.3	32.44	76.49	2.6	0.3	1.8	3.2
3	20181117	02:36:26.8	32.15	77.21	2.5	0.1	0.9	1.4
4	20181120	02:20:16.3	32.70	75.61	3.4	0.1	2.4	0.9
5	20181203	01:36:16.2	31.73	78.13	2.8	0.4	1.6	3.5
6	20181204	00:52:58.2	31.60	78.60	3.0	0.3	5.2	3.8
7	20181220	18:29:38.0	33.01	75.37	3.5	0.21	3.3	2.1
8	20181228	15:21:51.2	32.03	77.25	1.8	0.4	2.5	1.2
9	20190102	07:41:21.5	32.97	75.42	2.5	0.2	3.4	3.7
10	20190109	10:10:45.4	32.80	75.87	2.4	0.2	2.5	0.8
11	20190112	07:01:35.1	32.55	76.15	2.8	0.6	2.7	3.1
12	20190119	07:05:06.5	32.84	75.40	2.8	0.2	4.7	1.6
13	20190121	20:37:23.2	32.47	76.46	3.0	0.3	2.9	3.1
14	20190121	21:33:29.9	32.15	77.11	3.1	0.3	1.2	1.4
15	20190122	10:25:24.1	32.56	76.38	3.0	0.5	2.2	5.4
16	20190122	10:34:32.7	32.51	76.42	3.1	0.5	1.9	5.7
17	20190130	02:00:17.4	32.23	76.92	2.7	0.4	2.7	0.9
18	20190130	08:04:11.3	32.26	76.70	2.7	0.2	3.2	4.5
19	20190131	06:28:28.4	31.39	78.68	3.1	0.2	2.9	2.7
20	20190131	15:15:20.9	32.52	76.38	2.5	0.4	5.1	1.7
21	20190131	19:27:59.0	32.50	76.38	2.6	0.5	1.1	2.9
22	20190205	10:22:42.1	32.38	76.61	2.2	0.2	2.1	0.6
23	20190205	10:24:36.3	32.38	76.60	2.1	0.2	2.5	0.7
24	20190206	01:46:42.5	32.58	76.08	2.2	0.2	3.4	1.8
25	20190317	06:15:00.3	31.66	78.31	2.2	0.3	7.0	1.8

RESULTS

Figure 4 displays the locations of local events together with FPSs. The normal, reverse, and strike-slip faulting solutions are all displayed by FPSs, and it is evident that events that occur in close proximity to one another have distinct mechanisms. This happens because local events ($M<3.5$) typically have rupture lengths between a few hundred meters and one kilometer, and events might occur on faults that are oriented differently. From a total of 25 events, 3 events show normal faulting having both pure dip-slip component and left-lateral component, 19 events show reverse faulting with a left-lateral component, and 3 events show strike-slip mechanism. From the above discussion, Earthquakes depict all types of fault plane solutions. Interpretation of FPS concerning the T-axis and P-axis reveals the trend of direction. Orientations of the nodal planes, plunge and azimuth of the T-axis and P-axis, are tabulated in Tables 5 and 6.

DISCUSSION AND CONCLUSIONS

In this study, we investigated the focal mechanisms of 25 earthquakes in the Himachal Himalaya. We preferred the fault plane solutions with reliable P-wave first motions, because orientations of the fault planes and slip vectors are among the most crucial characteristics in the study of active tectonics of any region. Still, if more stations had recorded these events, the results would have been far more accurate. Tables 4, 5, and 6 provide the hypocenter and fault plane solution parameters. Figure 4 shows all types of solutions, and it is seen that events located very close to each other have different mechanisms. From a total of incidents, three exhibit normal faulting with a left-lateral component and a pure dip-slip component, nineteen exhibit reverse faulting with a left-lateral component, and three exhibit a strike-slip mechanism. The maximum concentration of thrust faults is consistent with the trend of the Himalayan collisional zone and the location of major faults.

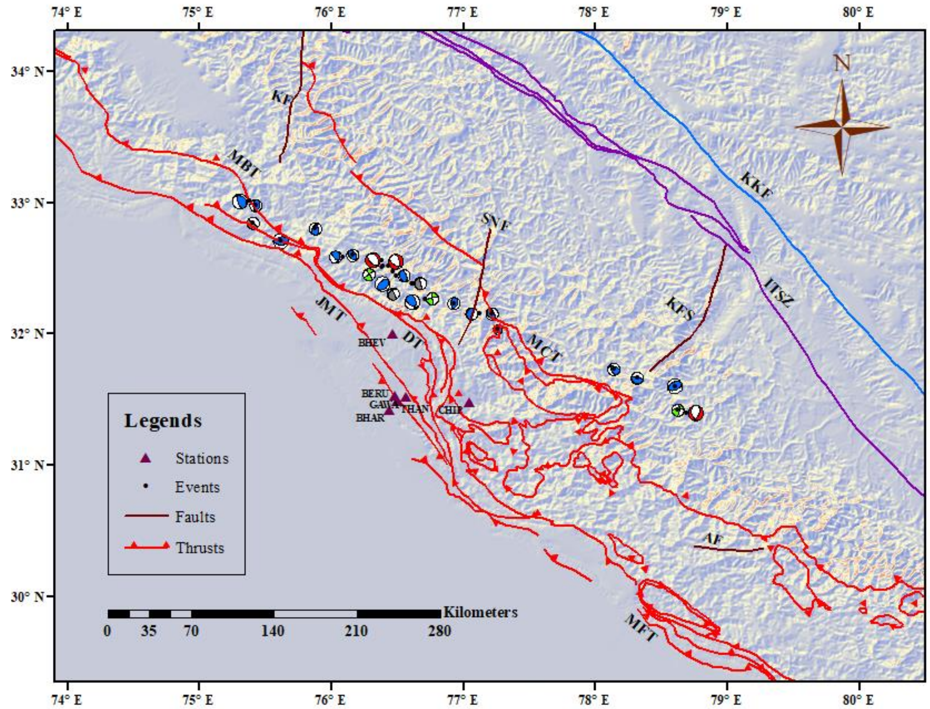

Figure 4. Beachball diagrams, in conjunction with the tectonic characteristics of the studied area, It allow for the deduction of focal mechanism solutions for well-located earthquakes based on P-wave polarity motion and amplitude ratio.

Table 5. Orientations of nodal planes obtained from FPS drawn for 25 events, Nodal plane-1 is identified as fault plane and Nodal plane-2 as auxiliary plane.

S. No.	Date (YYMMDD)	Lat (ºN)	Long (ºE)	Nodal plane-1			Nodal plane-2			Type of faulting
				Strike (deg.)	Dip (deg.)	Rake (deg.)	Strike (deg.)	Dip (deg.)	Rake (deg.)	
1	20181103	31.41	78.62	06	68	27	265.19	65.11	155.61	Strike-slip
2	20181111	32.44	76.49	160	32	90	340	58	90	Thrust fault
3	20181117	32.15	77.21	127	31	66	334.45	61.51	103.73	Thrust fault
4	20181120	32.70	75.61	258	45	79	93.37	46.04	100.80	Thrust fault
5	20181203	31.73	78.13	285	49	51	155.99	54.09	125.90	Thrust fault
6	20181204	31.60	78.60	244	42	89	65.35	48.01	90.90	Thrust fault
7	20181220	33.01	75.37	303	30	56	160.91	65.51	107.89	Thrust fault
8	20181228	32.03	77.25	260	54	59	125.63	46.10	125.33	Thrust fault
9	20190102	32.97	75.42	177	54	73	24.49	39.32	111.92	Thrust fault
10	20190109	32.80	75.87	341	52	53	211.75	51	127.61	Thrust fault
11	20190112	32.55	76.15	133	45	79	328.37	46.04	100.80	Thrust fault
12	20190119	32.84	75.40	312	86	89	146.05	4.12	104.01	Thrust fault
13	20190121	32.47	76.46	333	76	60	220.27	32.83	153.50	Thrust fault
14	20190121	32.15	77.11	200	20	90	20	70	90	Thrust fault
15	20190122	32.56	76.38	333	35	-75	134.89	56.36	-100.27	Normal fault
16	20190122	32.51	76.42	354	52	-53	123.25	51	-127.61	Normal fault
17	20190130	32.23	76.92	177	52	68	30.27	43.06	115.62	Thrust fault
18	20190130	32.26	76.70	170	89	-17	260.31	73	-178.95	Strike-slip
19	20190131	31.39	78.68	22	56	-64	160.90	41.84	-123.02	Normal fault
20	20190131	32.52	76.38	228	58	89	49.89	32.01	91.60	Thrust fault
21	20190131	32.50	76.38	326	84	8	235.16	82.04	173.94	Strike-slip
22	20190205	32.38	76.61	346	85	82	224.20	9.43	147.85	Thrust fault
23	20190205	32.38	76.60	122	52	53	352.75	51	127.61	Thrust fault
24	20190206	32.58	76.08	135	71	60	15.58	35.03	145.45	Thrust fault
25	20190317	31.66	78.31	281	78	85	123.82	12.99	112.30	Thrust fault

Table 6. Orientation of plunge and azimuth of T-axis and P-axis as obtained from FPS drawn for 25 events.

S. No	Date (YYMMDD)	Org time HR:MN:SS	Focal depth (Km)	P-axis		T-axis	
				Plunge (deg.)	Azimuth (deg.)	Plunge (deg.)	Azimuth (deg.)
1	20181103	11:08:08.2	22.5	1.88	135.08	34.23	46.36
2	20181111	21:50:09.3	7	13	250	77	70
3	20181117	02:36:26.8	14.4	15.87	234.40	69.85	93.62
4	20181120	02:20:16.3	5.4	0.53	355.75	82.23	261.90
5	20181203	01:36:16.2	33.4	02.82	41.46	61.48	306.26
6	20181204	00:52:58.2	16.3	3	334.71	86.92	167.29
7	20181220	18:29:38.0	7.1	18.62	57.66	64.89	281.70
8	20181228	15:21:51.2	32.2	4.29	11.42	64.96	290.65
9	20190102	07:41:21.5	13.9	07.55	279.04	74.30	217.18
10	20190109	10:10:45.4	10	0.55	96.19	61.68	7.21
11	20190112	07:01:35.1	0.1	0.53	230.75	82.23	136.90
12	20190119	07:05:06.5	17	40.99	42.94	48.99	40.92
13	20190121	20:37:23.2	7	25.03	85.97	49.93	29.69
14	20190121	21:33:29.9	18	25	290	65	110
15	20190122	10:25:24.1	6.1	76.16	193.06	10.81	52.26
16	20190122	10:34:32.7	8.6	61.68	147.79	0.55	58.81
17	20190130	02:00:17.4	2.2	4.66	282.41	72.17	207.10
18	20190130	08:04:11.3	43.1	12.65	303.87	11.21	216.42
19	20190131	06:28:28.4	22.3	67.26	165.33	7.56	93.78
20	20190131	15:15:20.9	6.1	12.99	318.73	76.98	314.86
21	20190131	19:27:59.0	0.6	1.37	100.46	9.89	10.70
22	20190205	10:22:42.1	9.9	39.49	83.33	49.39	67.30
23	20190205	10:24:36.3	10	0.55	237.19	61.68	148.21
24	20190206	01:46:42.5	2.4	20.41	247.16	54.02	188
25	20190317	06:15:00.3	26.2	32.82	15.21	56.72	4.55

Previous studies suggested that the Ropar-Manali fault, earlier recognized as a lineament, shows dextral strike-slip motion and is transverse to the regional Himalayan strike. The fault extends from Ropar through Sundarnagar, Mandi, and Kullu to Manali in Himachal Pradesh. An earthquake with strike-slip motion is close to the Sundarnagar fault. There may be a genetic relationship between the Himalayan block above the MBT and a transverse structural feature in the underthrusting Indian plate (Sundarnagar fault). The MCT and MBT are tectonically analogous faults of various ages. Some earthquakes show normal faulting above the MCT, and some thrust events are very close to the west and east sides of the MBT. Therefore, considering the orientation of fault planes in the beachball representation of the fault plane solutions, they are oriented with the Himalayan thrusts and faults. Tandon and Srivastava (1975) conducted an investigation for three regions, namely Kashmir, Central Himalaya and northeast India, including Assam. They determined the fault plane solutions of 30 events. From theses events, 4 events show normal faulting, 25 events show reverse faulting with a left-lateral component, and 1 event shows a strike-slip mechanism. Molnar and Deng (1984) conducted an investigation into the faulting process associated with large earthquakes and the corresponding average deformation rates across Central and Eastern Asia. Their analysis demonstrated that the majority of the large earthquakes are characterized by thrust faulting, a finding that aligns well with the results of the present study.

The direction of the trend is revealed by interpreting FPS in relation to the T- and P-axes. According to the T-axis, 10 events have azimuths between 4.55^0 to 70^0 that trend in the north-east direction, 6 events have azimuths between 93.62^0 to 167.29^0 that trend in the south-east direction, 5 events have azimuths between 188^0 to 261.90^0 that trend in the south-west direction, and 4 events have azimuths between 281^0 to 314.86^0 that trend in the north-west direction, respectively. According to the P-axis, 6 events have azimuths between 193^0 to 250^0 that trend in the south-west direction. P-axis azimuths of 5 events vary from 96.19^0 to 165.33^0 that trend in the south-east direction. Remaining, each 7 events have azimuths between 11.42^0 to 85.97^0, and 279.04^0 to 355.75^0 that trend in north-east and north-west directions, respectively.

Acknowledgments

The authors are grateful to the organizations and individual sections that provided the data and information used in the present study. The authors express their gratitude to the Department of Earthquake Engineering, IIT Roorkee, for providing the data and research facilities. The authors are appreciative of their support.

Author credit statement

Ankush Kumar Ruhela has done the formal analysis and research work presented in this paper using Seisan software for focal mechanisms. J. Das and S.C. Gupta supervised the whole research work and helped in the planning and execution of the manuscript. All the named authors provided their critical feedback on data interpretation and supported the improvement of the manuscript.

Data Availability

The data used in the study is provided by the Department of Earthquake Engineering, IIT Roorkee, India.

Compliance with ethical standards

The authors declare that there are no known financial conflicts of interest or personal relationships that could have influenced the work presented in the paper. They adhere to copyright norms

References

Barazangi, M. and Ni, J., 1982. Velocities and propagation characteristics of Pn and Sn beneath the Himalayan arc and Tibetan plateau: Possible evidence for underthrusting of Indian continental lithosphere beneath Tibet. Geology, 10(4), 179-185.

Bird, P., 1978. Initiation of intracontinental subduction in the Himalaya. J. Geophys. Res.,Solid Earth, 83(B10), 4975-4987.

Castillo, D.A. and Ellsworth, W.L., 1993. Seismotectonics of the San Andreas Fault system between Point Arena and Cape Mendocino in north California: Implications for the development and evolution of a young transform. J. Geophys. Res., 98, 6543-6560.

Chander, R., Sarkar, I., Khattri, K. N. and Gaur, V. K., 1986. Upper crustal compressional wave velocity in the Garhwal Himalaya. Tectonophysics, 124, 133–140.

Cotton, F., Campillo, M., Deschamps, A. and Rastogi, B. K., 1996. Rupture history and seismotectonics of the 1991 Uttarkashi, Himalaya arthquake. Tectonophysics, 258(1-4), 35-51.

Cronin, V.S., 2010. A primer on focal mechanism solutions for geologists. Science Education Resource Center, Carleton College, http:serc.carleton.edu/files/NAGT workshops/ structure 04/focal_mechanism_primer.pdf.

Dewey, J. F. and Bird, J. M., 1970. Mountain belts and the new global tectonics. J. Geophys. Res., 75(14), 2625-2647.

GSI, 2000. Geological Survey of India, Seismotectonic atlas of India and its environs.

Hauksson, E., 1990. Earthquakes, faulting, and stress in the Los Angeles basin. J. Geophys. Res., Solid Earth, 95(B10), 15365-15394.

Havskov, J. and Ottemoller, L., 2003. SEISAN: the earthquake analysis softwares for windows, Solaris and Linux, version 8.0. Norway: Institute of Solid Earth Physics, University of Bergen.

Hodgson, J. H., 1957. The nature of faulting in large earthquakes. Bull. Geol. Soc. Am., 68, 611- 644.

Honda, H., Masatsuka, A. and Emura, K., 1956. On the mechanism of the earthquakes and the stress producing them in Japan and its vicinity. Sic Rep. Tohoku University, Set. 5, 8, 186-205.

Isacks, B.L. and Molnar, P., 1971. Distribution of stresses in the descending lithosphere from a global survey of focal-mechanism solutions of mantle earthquakes, Rev. Geophys., 9, 103-174.

Isacks, B., Oliver, J. and Sykes, L. R., 1968. Seismology and the new global tectonics. J. Geophys. Res., 73(18), 5855-5899.

Ishida, M., 1992. Geometry and relative motion of the Philippine Sea plate and Pacific plate beneath the Kanto-Tokai district, Japan. J. Geophys. Res., 97, 489-513.

Kumar, A., Pandey, A.D., Sharma, M.L., Gupta, S.C., Verma, A.K., and Gupta, B.K., 1994. Processing and preliminary interpretation of digital data obtained from a digital seismic array in Garhwal Himalaya. Symposium on Earthquake Engineering, University of Roorkee, India, Vol. 1, 141-152.

LeFort, P., 1975. Himalayas: The collided range, present knowledge of the continental arc: Am. J. Sci., 275-A, 1-44.

Lienert, B.R. and Havskov, J., 1995. A computer program for locating earthquakes both locally and globally. Seism. Res. Lett., 66 (5), 26-36.

McIntyre, D. B. and Christie, J., 1957. A discussion of "The nature of Faulting in Large Earthquakes". Bull. Geol. Soc. Am., 68, 645-652.

McKenzie, D. P. and Parker, R. L., 1967. The North Pacific: an example of tectonics on a sphere. Nature, 216, 1276-1280.

Molnar, P. and Chen, W. P., 1983. Focal depths and fault plane solutions of earthquakes under the Tibetan Plateau. J. Geophys. Res., 88, 1180 – 1196.

Molnar, P. and Qidong, D., 1984. Faulting associated with large earthquakes and the average rate of deformation in central and eastern Asia. J. Geophys.Res.,Solid Earth, 89(B7), 6203-6227.

Molnar, P., Chen, W. P., Fitch, T. J., Tapponnier, P., Warsi, W. E. K. and Wu, F. T., 1977. Structure and tectonics of Himalaya: A brief summary of relevant geophysical observations, Colloq. Int CNRS, Ecologie et Geologic de the Himalaya, Vol. 268, 269-294.

Morgan, W. J., 1968. Rises, trenches, great faults, and crustal blocks. J. Geophys. Res.,73, 1959- 1982.

Ndikum, E.N., Tabod, C.T., Tokam, A.K. and Essimbi, B.Z., 2014. Fault-plane solution of the earthquake of 19 march 2005 in Monatele (Cameroon). Open J. Geology. 4, 289-293.

Powell, C. M. and Conaghan, P. J., 1973. Plate tectonics and the Himalayas. Earth and Planet. Sci. Lett., 20(1), 1-12.

Scheidegger, A. E., 1964. The tectonic stress and tectonic motion direction in Europe and Western Asia as calculated from earthquake fault plane solutions. Bull. Seism. Soc. Am., 54, 1519-1528.

Seeber, L., Quittmeyer, R. and Armbruster, J.G., 1981. Seismicity and continental subduction in the Himalayan arc, in Zagros, Hindu Kush, Himalaya, Geodynamic Evolution, Geodyn. Ser., vol. 3, edited by H.K. Gupta and F.M. Delany, pp. 215-242, AGU, Washington, D.C.

Shirokova, E. I., 1967. General features in the orientation of principal stresses in earthquake foci in the Mediterranean-Asian seismic belt. Izv. Akad. Naul~ S.S.S.R. (Physics of the Solid Earth) 12-22 (English translation).

Snoke, J.A., Munsey, J.W., Teague, A.C. and Bollinger, G.A., 1984. A program for focal mechanism determination by combined use of polarity and Sv-P amplitude ratio data, Earthquake notes, 55-3-15.

Stauder, W., 1964. A comparison of multiple solutions of focal mechanisms. Bull.Seism. Soc. Am., 54, 927-937.

Tandon, A. N. and Srivastava, N., 1975. Fault plane solutions as related to known geological faults in and near India. Annals of Geophys., 28(1), 14-27.

Wickens, A.J. and Hodgson, J.H., 1967. Computer re-evaluation of earthquake mechanism solutions. Publ. Dom. Obs. Ottawa, 33(1), 1-560.

Xu, W., Burgmann, R. and Li, Z., 2016. An improved geodetic source model for the 1999 Mw 6.3 Chamoli earthquake, India. Geophys. J. Int., 205, 236–242. https://doi.org/10.1093/gji/ggw016.

Yamazaki, F., Horiuchi, S., Ito, K. and Moriya, T., 1992. Focal Mechanism Analyses of Aftershocks of the 1984 Western Nagano Prefecture Earthquake. J. Phys. Earth, 40, 327-341.

Received on: 9-10-2024; Revised on: 29-11-2025; Accepted on: 30-11-2025